A neurophysiological–metabolic model for burst suppression

ShiNung Ching[a,b,1], Patrick L. Purdon[a,b,c], Sujith Vijayan[d], Nancy J. Kopell[d,1], and Emery N. Brown[a,b,c,e]

[a]Department of Anesthesia, Critical Care and Pain Medicine, Massachusetts General Hospital, Boston, MA 02114; [b]Department of Brain and Cognitive Science, and [e]Harvard–Massachusetts Institute of Technology Division of Health Sciences and Technology, Massachusetts Institute of Technology, Cambridge, MA 02139; [c]Harvard Medical School, Cambridge, MA 02115; and [d]Department of Mathematics and Statistics, Boston University, Boston, MA 02215

Contributed by N. Kopell, December 27, 2011 (sent for review November 18, 2011)

Burst suppression is an electroencepholagram (EEG) pattern in which high-voltage activity alternates with isoelectric quiescence. It is characteristic of an inactivated brain and is commonly observed at deep levels of general anesthesia, hypothermia, and in pathological conditions such as coma and early infantile encephalopathy. We propose a unifying mechanism for burst suppression that accounts for all of these conditions. By constructing a biophysical computational model, we show how the prevailing features of burst suppression may arise through the interaction between neuronal dynamics and brain metabolism. In each condition, the model suggests that a decrease in cerebral metabolic rate, coupled with the stabilizing properties of ATP-gated potassium channels, leads to the characteristic epochs of suppression. Consequently, the model makes a number of specific predictions of experimental and clinical relevance.

Burst suppression—an electroencephalogram (EEG) pattern in which high voltage activity (burst) and flatline (suppression) periods alternate systematically but quasiperiodically (almost periodic but with variations in inter- and intra-burst duration) (1)—is a state of profound brain inactivation. It is frequently observed in deep general anesthesia (2). It is also observed in a range of pathological conditions including hypothermia (3–5), hypoxic–ischemic trauma/coma (6), and the so-called Ohtahara syndrome (7, 8), a type of early infantile encephalopathy. These etiologies indicate that the burst suppression pattern represents a low-order dynamic mechanism that persists in the absence of higher-level brain activity. Indeed, the fact that many different conditions produce similar brain activity suggests that there may be a common pathway to the state of brain inactivation and may indicate fundamental properties of the brain's arousal circuits (2).

The basic features of the burst suppression phenomenon have been established through a variety of EEG studies that are reviewed in ref. 9. The two most notable of these features are the spatial homogeneity of bursts and the quasi-periodic nature of the suppression. Later research has been directed at describing the phenomenon in vivo and in the specific context of general anesthesia. In particular, the early work of Steriade et al. (10) helped establish the neural correlates of burst suppression, including the differential participation of cortical and subcortical cell types. More recent studies (11, 12) have suggested that burst suppression is associated with enhanced excitability in cortical networks. These studies implicate extracellular calcium as a correlate for the switches between burst and suppression.

Despite the findings of these studies, a unifying mechanism for burst suppression—one that explains its prevailing features and also accounts for its range of etiologies—has not been proposed. Indeed, the existing characterizations of burst suppression in pathological situations are highly limited. Computational models offer a means of synthesizing the available data with known physiology to propose potential mechanisms and predictions that may guide future experiments. Such is the objective of this paper. Previous attempts at modeling burst suppression have been largely phenomenological (13), using arguments from chaos theory to explain certain properties of the burst suppression waveform. These models do not clarify the underlying biophysical dynamics.

In contrast, we construct a biophysical model that is constrained by neurophysiology and the commonality between the aforementioned etiologies—specifically, a reduction in brain metabolism. The unique feature of our model is a nuanced interaction between neuronal dynamics and changes in cerebral metabolic rate of oxygen (CMRO). The model produces the distinctive characteristics of burst suppression, providing unique insights and predictions regarding low-order brain dynamics in states of reduced activity. Specifically, it suggests that burst suppression represents a basal neurometabolic regime that ensures basic cell function during states of lowered metabolism. We discuss clinical and experimental implications of these findings.

Prevailing Features of Burst Suppression

To constrain the model, we first consider three prevailing features of burst suppression, summarized in refs. 6 and 9, for which there is clinical and experimental evidence. The first feature of note is the synchrony of burst onset; (i.e., bursts begin and end nearly simultaneously across the entire scalp). Such a spatially homogeneous behavior immediately suggests that a very low-order dynamic mechanism underlies burst suppression. Some studies have suggested that asynchronous burst suppression can arise in the case of large-scale cortical deafferentation (14, 15). In such settings, large-scale differences in regional blood supply and autoregulation may prevent the uniformity typically associated with burst suppression.

A second important feature of burst suppression is its parametric sensitivity to the level of brain depression—for instance, depth of general anesthesia. In particular, the burst suppression ratio (BSR)—the fraction of time spent in suppression—is known to increase as general anesthesia deepens (16). Eventually, with sufficient quantities of drug, a completely isoelectric (flatline) EEG can be achieved. A similar progressive increase in BSR can be observed during hypothermia (see below). Thus, the burst suppression pattern is not a discrete state, but occurs on a continuum guided by a changing underlying biophysical process.

Finally, we note the significant difference in timescales between burst suppression and other neural activity associated with an inactivated brain state, specifically, the 0.5- to 2-Hz slow/delta oscillation commonly observed during sleep and general anesthesia. Burst suppression occurs on a much slower timescale than these oscillations. Bursts may last multiple seconds interspersed with as long as 10–20 s of suppression (Fig. 1*A* and Fig. 2).

Author contributions: E.N.B., N.J.K., and S.C. designed modeling research; E.N.B. and P.L.P. designed experimental research; S.C. and P.L.P. performed research; S.V. contributed model concepts and parameterizations; S.C. and P.L.P. analyzed data; and S.C., E.N.B., and N.J.K. wrote the paper.

The authors declare no conflict of interest.

[1]To whom correspondence may be addressed. E-mail: shinung@neurostat.mit.edu or nk@bu.edu.

This article contains supporting information online at www.pnas.org/lookup/suppl/doi:10.1073/pnas.1121461109/-/DCSupplemental.

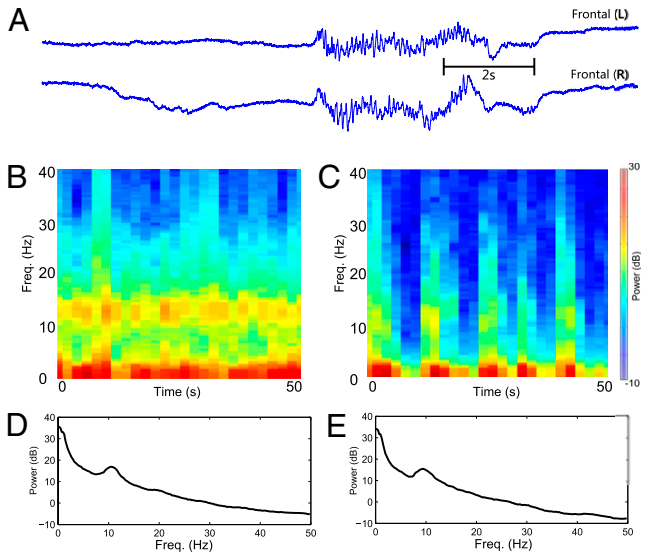

Fig. 1. Burst suppression phenomenology. (*A*) A typical recording of burst suppression from a human subject anesthetized with propofol–general anesthesia. The bursts manifest concurrently across the scalp (here, shown for left and right frontal electrodes). (*B*) Spectrogram for a frontal electrode during deep, but not burst-suppression, general anesthesia. The alpha rhythm associated, described in ref. 19, is manifest. (*C*) At a deeper level of general anesthesia, burst suppression is achieved (the spectrogram clearly displays epochs of quiescence). When a burst occurs, the alpha activity is recovered. (*D*) Alpha peak during deep, but not burst-suppression, general anesthesia. Spectrum was averaged from 25 4-s epochs. (*E*) Alpha peak during burst suppression. Spectrum was averaged from 25 burst epochs.

Moreover, unlike slow oscillations, burst suppression is not periodic (17). Indeed, it has been suggested that slow oscillations are contained within bursts (11), indicating that burst suppression may be governed by a more global dynamic process.

Additional Data and Constraints

To develop additional constraints, we examine burst suppression EEG recordings from healthy volunteers anesthetized with the widely used anesthetic propofol. These recordings were collected as part of a larger study on the electrophysiological and behavioral effects of propofol general anesthesia (18).

Fig. 1*A* shows a representative epoch of burst suppression from left- and right-frontal electrodes from such a subject. As is typical in burst suppression, the bursts begin and end synchronously between hemispheres. Fig. 1*B* shows the spectrogram of a frontal electrode at a deep, but not burst suppression, level of general anesthesia. As has been described in refs. 19 and 20 and shown in Fig. 1*B*, this level of general anesthesia is characterized by a persistent, high-power alpha rhythm in the 10- to 13-Hz range. Fig. 1*C* shows a spectrogram of the same electrode when the anesthetic dose is increased to a level sufficient to produce burst suppression. The suppression epochs are clearly observed as broadband reductions in power. Importantly, however, during the burst epochs, the alpha rhythm persists (see also Fig. 1 *D* and *E*, which shows the average spectra for the pre-burst suppression and burst suppression phases of the infusion, respectively). Morphologically, it is as if Fig. 1*B* has been multiplied by an alternating sequence of zeros and ones.

This observation provides an important insight: The mechanisms for alpha rhythmogenesis survive the onset of burst suppression. A similar feature has been observed during burst suppression induced by isoflurane general anesthesia, in which slow-wave and delta activity persists during the burst epochs (11). The propofol-induced alpha is thought to involve potentiation of gamma aminobutyric acid (GABA) inhibitory currents in thalamocortical loops (20, 21). The recovery of these mechanisms during bursts suggests that a more global dynamic perturbation, (i.e., not simply an increase in GABA, must be responsible for creating the epochs of suppression).

Approach: A Link to Metabolism

To develop a modeling approach that accounts for the above features, we look to the common aspects of the different burst suppression etiologies—specifically, their relationship to aberrant neurometabolic dynamics. Clearly, hypoxic–ischemic coma is associated with severe changes to brain metabolism and CMRO (6, 22). Early infantile encephalopathy that is not directly linked to a hypoxic–ischemic event, [e.g., Ohtahara's syndrome (7, 8)], is nevertheless associated with brain atrophy and metabolic dysfunction (23).

A reduced CMRO is also characteristic of burst suppression during hypothermia (3), [i.e., brain cooling, which is frequently used to induce or maintain medical coma during surgeries that involve circulatory arrest (4, 24) or for cerebral protection after cardiac arrest]. An example of this is shown in Fig. 2, which shows a frontal EEG from a patient undergoing circulatory rewarming after induced hypothermia during cardiac surgery (*SI Methods*). As rewarming occurs, the BSR decreases until a continuous EEG is recovered. This gradual decrease in BSR is similar to the progression observed during emergence from general anesthesia. In the context of anesthetic drugs, it is known that most intravenous GABAergic induction agents lead to significantly reduced CMRO (25). Those that are associated with increased CMRO, such as ketamine, do not lead to the classical pattern of burst suppression at clinically relevant dose levels (26).

This evidence suggests a link between reduced cerebral metabolism and the state of burst suppression. At the neuronal network level, a candidate for providing this link is the adenosine trisphosphate (ATP)-gated potassium channel (K_{ATP}), which is thought to provide neuronal protection during hypoxic–ischemic events (27, 28). It has been shown that, in certain cortical areas, this channel may lead to very slow (<0.5 Hz) oscillatory activity (29). The involvement of this channel—or one similar in behavior—in burst suppression is investigated in the subsequent sections of this paper.

Objectives

We seek a biophysical model that accounts for the following features of burst suppression: (*i*) the quasiperiodic onset and offset of bursts across the scalp; (*ii*) the very slow timescales associated with burst and suppression duration; (*iii*) the parametric modulation of BSR as a function of anesthetic dose, hypothermia, or metabolic reduction; and (*iv*) the association of burst suppression with states of lowered cerebral metabolism.

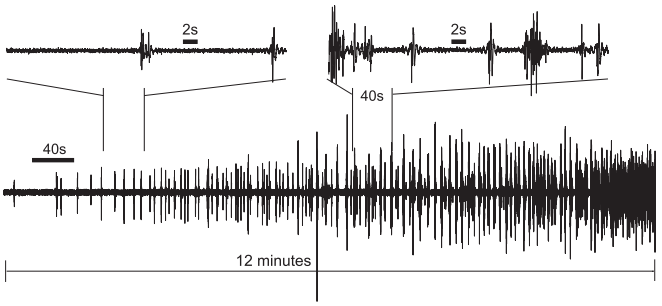

Fig. 2. Burst suppression in frontal EEG of a human undergoing circulatory rewarming following hypothermic cardiac surgery. Patient was cooled to a peak hypothermic temperature of 18 °C before eventual rewarming. Observe the gradual decrease in BSR as temperature increases until continuous electrical activity is recovered. Two 40-s detailed epochs are shown.

Methods

Model Structure. We construct a model consisting of biophysical cortical neurons that are described by voltage-gated conductance equations of the Hodgkin–Huxley type (30). The primary feature of the model is the aforementioned K_{ATP} channel, which modulates neuronal firing as a function of ATP production. The rate of ATP production is, in turn, directly modulated by CMRO (31, 32). The schematic of the model is shown in Fig. 3. The neuronal network consists of cortical pyramidal neurons and interneurons that produce neuronal oscillations on timescales commensurate with the EEG observed during general anesthesia (19, 20). To this network, we add dynamics associated with ATP consumption, in the form of the sodium–ATP pump, which is thought to be the major consumer of cerebral ATP (29, 33). Changes to the rate of ATP production can be related to each of the etiologies of burst suppression (Fig. 3*B*). In the case of general anesthesia, down-regulation of neuronal firing through enhanced synaptic inhibition will lead to an autoregulatory decrease in CMRO (25). Other physiological perturbations, such as hypothermia or hypoxic/ischemic injury, may directly down-regulate brain metabolism without changing synaptic properties (3, 6). For the purposes of our modeling study, we manipulate the rate of ATP production as a free parameter.

In the model, all cells are described using differential equations of the form

$$c_m \dot{V} = -\sum I_{\text{memb}} - \sum I_{\text{syn}} + I_{\text{app}}, \quad [1]$$

where I_{memb} and I_{syn} are membrane and synaptic currents, respectively, and I_{app} represents random external noise. We illustrate the main results using small networks of two principal cell types, cortical pyramidal cells and inhibitory interneurons. We consider model networks of up to 20 cells.

The link to metabolic dynamics comes through the ATP-gated potassium membrane current, $I_{K_{ATP}}$, which is a component of I_{memb} in [1] and is defined by

$$I_{K_{ATP}} = g_{K_{ATP}} z (V - E_K), \quad [2]$$

where $g_{K_{ATP}}$ is the channel conductance, V is the membrane potential and E_K is the potassium channel reversal potential. The gating variable z is $z = (1 + 10[ATP])^{-1}$, defined in terms of the ATP concentration [ATP], which itself is governed by the exchange of sodium and ATP (29, 34):

$$\begin{aligned} \left[\dot{Na}\right] &= F \cdot I_{Na} - 3K_m [Na]^3 [ATP] \\ \left[\dot{ATP}\right] &= J_{ATP}([ATP]_{\max} - [ATP]) - K_m [Na]^3 [ATP]. \end{aligned} \quad [3]$$

Here, the kinetic constants F and K_m govern the Na–ATP pump dynamics. The parameter J_{ATP} is the production rate of ATP that is known to be directly coupled to the cerebral metabolic rate (32). As a surrogate for the metabolic rate, we directly manipulate J_{ATP} over a range of 30–50% of baseline, consistent with studies of anesthetic and hypothermic effects on cerebral metabolism (35, 36). Complete details of the model and simulation parameters are found in *SI Methods*.

Results

Metabolic Dynamics Lead to Burst-Like Phenomena. We demonstrate the main result using a purely cortical network consisting of reciprocally coupled interneurons and pyramidal cells. As shown previously (20, 37), such a network can be used to explain the progressive reduction in frequency of EEG oscillations observed during induction of general anesthesia via propofol. The mechanism in those models was a drug-induced potentiation of $GABA_A$ inhibitory postsynaptic potentials. Here, we build upon these models by adding metabolic dynamics.

Fig. 4 shows the simulated local field potential (LFP) obtained from a network of 14 cells—10 pyramidal cells and 4 interneurons—for baseline and lowered levels of ATP regeneration, respectively. The traces are from a representative simulation but are repeatable and robust to model noise. As is shown, when the ATP regeneration is lowered to 50% of baseline, continuous neural activity gives way to epochs of quiescence. Bursts and suppression epochs are on the order of 4–10 s and alternate quasiperiodically. When ATP regeneration is lowered further to 30% of baseline (Fig. 4*C*), a notable increase in the BSR occurs. Fig. S1 shows the computed BSR as a function of J_{ATP} over the 30–50% range. From Fig. S1 we note that the length of bursts becomes more variable as J_{ATP} increases.

The mechanisms that underlie this phenomenon can be established using a minimal network consisting of only a single pyramidal cell and a single interneuron. Using this configuration, Fig. 5 shows the output of a cortical pyramidal neuron for 50% and 30% reductions in ATP regeneration rate. Fig. 5*A* shows the bursting activity, where the spiking within the bursts has alpha periodicity, consistent with ref. 20. The transition from burst to suppression can be understood in terms of the intracellular ATP concentration $[ATP]$. As shown in Fig. 5*B*, as a burst occurs, $[ATP]$ decreases by ~25%. This decrease causes an increase in the conductance $g_{K_{ATP}}$ (9) as shown in Fig. 5*C*. The opening of the K_{ATP} channel leads to hyperpolarization and prohibits further spiking. During the suppression, $[ATP]$ slowly recovers according to ref. 10, lowering $g_{K_{ATP}}$ until spiking is once again facilitated.

The quasiperiodicity in Fig. 4 arises from parametric variation within the population of principal cells, along with a small amount of random background activity, which is consistent with ongoing time-varying afferent input to a cortical population (38). In effect, the network inhomogeneity, along with the noise, causes bursts to be initiated at variable times during the recovery of $[ATP]$ (note the time course of $[ATP]$ in Fig. 5). In the small model with no noise the burst suppression pattern is more regular and periodic. Fig. S1 shows the cross-covariance of the simulated LFP for the range 30–50% J_{ATP}, where the quasiperiodicity is reflected by the dominant peak at 0-s lag and the weak side peaks. The variation in interburst timing may also be affected by slow processes such as cerebral blood flow (39), although such factors are not explicitly included in this model.

Spectral Content Is Preserved Within Bursts. The model confirms that spectral content remains intact within burst epochs. Fig. 6 shows the spectrograms of the simulations of baseline and burst-suppression activity. In Fig. 6*A* we see the 10- to 12-Hz alpha

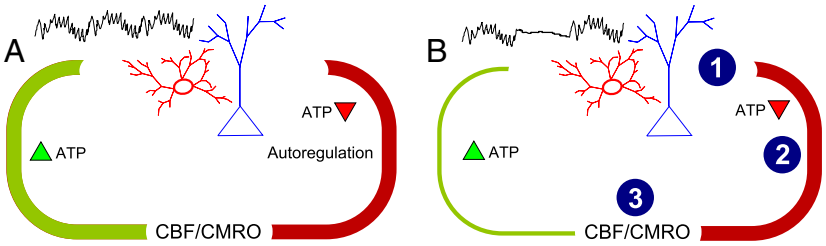

Fig. 3. Schematic of model system. Cortical interneurons and pyramidal cells interact to produce oscillations through previously established mechanisms (15, 34). The dynamics of ATP coupled with CMRO modulate these oscillations in a manner that produces burst-suppression morphology. (*A*) In a normal metabolic regime, ATP production is coupled to flow and CMRO through normal autoregulatory mechanisms. (*B*) When production is compromised, deficiencies in ATP lead to activation of K_{ATP} channels and, consequently, periods of quiescence. Such perturbations may arise through multiple etiologies: (*1*) Anesthetics may down-regulate neuronal spiking activity, leading to decreased metabolic demand; (*2*) autoregulatory mechanisms modulate metabolism in response to changes in neural activity; and (*3*) cerebral blood flow or metabolic rate may be down-regulated exogenously due to hypothermia or injury.

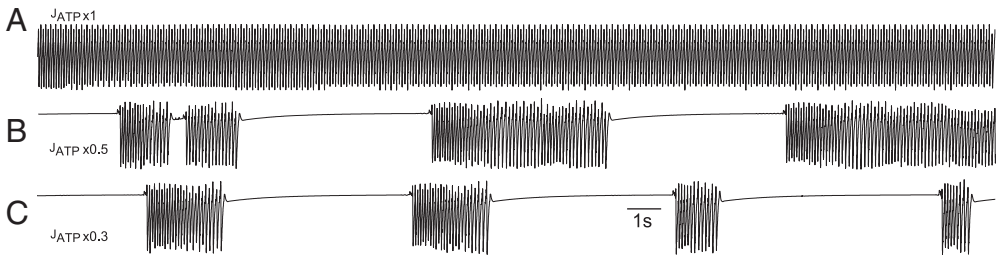

Fig. 4. Model produces suppression-like activity. The three traces show simulated LFP from a population of cortical cells under different metabolic parameterizations. (*A*) Baseline metabolic rate produces sustained, periodic output consistent with a deep (but not burst-suppression) level of general anesthesia. (*B*) A 50% reduction in production rate leads to an ~0.5 BSR. (*C*) A further decrease to 30% production rate leads to a 0.75 BSR.

oscillation that is associated with surgical levels of general anesthesia (20). In Fig. 6*B*, we see that this alpha activity persists during the burst intervals. The phenomenon is again due to the underlying dynamics of the K_{ATP} channel. As shown in Fig. 5*B*, during the periods of activity, $g_{K_{ATP}}$ operates near baseline. Consequently, the neuronal network operates in a normal dynamic range and thus the alpha oscillation is recovered. As the burst progresses, $g_{K_{ATP}}$ eventually moves away from baseline, leading to intraburst frequency variations. Such variability is studied below.

Spectral Drift Within Burst. The model exhibits an interesting emergent phenomenon: a progressive slowing in frequency toward the end of a burst. Fig. 7 shows the spectrogram of a 40-s period of burst suppression generated from the model using a parameterization for 30% reduction in ATP production. Here, bursts are 4–6 s in duration. Note that the frequency within each burst slowly decreases from an initial value >10 Hz to a final value near 8 Hz.

As such, the model suggests that the burst suppression morphology is not simply that of an "on–off" switching function. Indeed, the activity appears to wax and wane, with a notable reduction in frequency toward the end of a burst. As seen in Fig. 5, this behavior can be attributed to the slow variation in the K_{ATP} channel as the burst progresses. As $g_{K_{ATP}}$ increases, the pyramidal cell transitions through a regime where spiking occurs but is slowed. Such dynamics are analogous to calcium fluctuations in certain thalamic cells, (i.e., so-called calcium bursts), but on a much slower and irregular timescale. They are a novel property of this model and have yet to be verified in experimental data.

Limits in High-Frequency Intraburst Activity. The model predicts limitations to high-frequency neuronal activity during a compromised metabolic regime. Fig. 8 shows the maximum frequency of action potential firing for a pyramidal cell from the model as a function of the time constant and conductance of GABA-ergic inhibition. Note that a 3–4× potentiation in GABA is consistent with common general anesthetics (20) (1× corresponds to an unanesthetized baseline). When the model is parameterized with baseline values of ATP production, the timescale of inhibition sets the firing rate of the network (and of this pyramidal cell) (38), leading to a progressive reduction in firing from the gamma to the alpha range. Fig. 8 also shows the frequency output over the same range of GABA potentiation for a 30% reduction in J_{ATP}. In this scenario, the network produces burst suppression. However, *within* each burst the spiking frequency is restricted to the 10-Hz range; (i.e., high-frequency firing is impeded by metabolic modulation and not through inhibitory synaptic effects).

Discussion

Neuronal–Metabolic Model for Burst Suppression. We have developed a model for burst suppression that combines effects at the local circuit level with broader effects on neural metabolism. In the model, the link between these two levels of physiology is through the ATP-gated potassium channel, which is known to be expressed in cortex and subcortical structures (28). Activation of this channel serves to stabilize cell membranes, leading to seconds-long periods of alternating activity and suppression.

It is known that altered neurometabolic dynamics can occur in each of the conditions associated with burst suppression: in general anesthesia, through a reduction in neural activity and subsequent reductions in CMRO (25, 36); in hypoxic/ischemic injury, through aberrant reductions in metabolic regulation due to diffuse injury or through direct oxidative stress (6, 22); in hypothermia, through direct reductions in metabolic rate (3, 35); and in developmental encephalopathy, through neural and metabolic dysfunction (23). Implicating brain metabolism in the neural mechanisms of burst suppression establishes a unifying physiologic connection between the main etiologies of the phenomenon.

The model provides an explanation of the central features of burst suppression: (*i*) The progressive and continuous increase in BSR with deeper levels of inactivation is due to a progressive reduction in metabolism, for instance through a decrease in CMRO; (*ii*) the spatial synchrony of burst onset and offset may arise through the broad manifestation of such metabolic changes, including in subcortical structures (noting that the present model is spatially compact); and (*iii*) the recovery of rhythms within bursts is due to recovery of basal dynamics at the neuronal circuit level caused by transient increases in energetics.

In addition, the model suggests new phenomenological features: (*iv*) a drift in the rhythmic activity through the course of a burst due to slow depletion and subsequent increase in $g_{K_{ATP}}$ and (*v*) a limitation in high-frequency intraburst activity independent of the strength of synaptic inhibition.

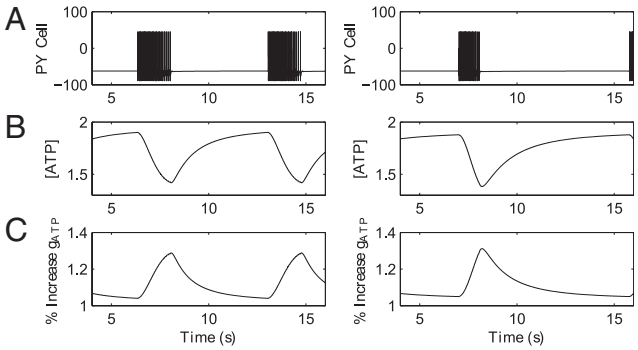

Fig. 5. Mechanism associated with burst activity for 50% (*Left*) and 30% (*Right*) J_{ATP}. (*A*) A pyramidal cell in a minimal network configuration spikes with interspersed periods of quiescence. (*B*) During spike epochs, ATP levels are depleted due to compromised metabolism. Once activity ceases, ATP levels slowly regenerate until activity can once again be sustained. (*C*) Increase (× baseline) in the conductance of the K_{ATP} channel. Large increases in g_{ATP} (due to activity-dependent depletion) lead to cessation of spiking.

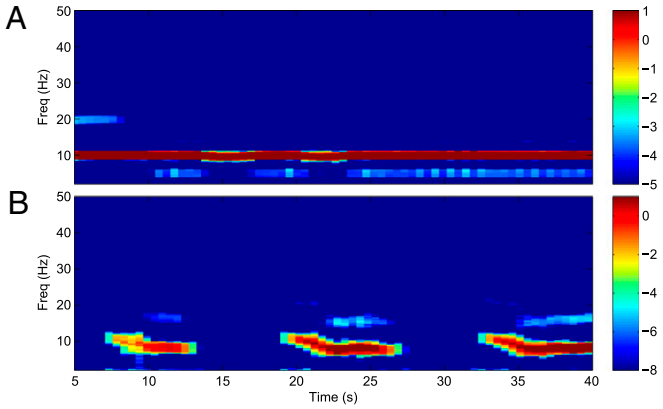

Fig. 6. Spectral content is preserved within bursts. (*A*) In a baseline metabolic regime, the model produces persistent alpha activity. This is a spectrogram of Fig. 1*A*. (*B*) In a 50% reduced metabolic regime, the model produces burst suppression. Within each burst, the alpha activity is recovered. This is a spectrogram of Fig. 1*B*.

Consistency with Previous Studies. The model is consistent with descriptions of burst suppression in general anesthesia, hypoxic–ischemic brain injury, and childhood encephalopathy (25). At the cellular level, the model is compatible with ref. 10, which showed wide synchrony of bursts and a strong correlation between cortical spiking and burst activity as measured by field potentials. The fact that some subcortical cells produce spikes during cortical quiescence may be due to differential expression of the K_{ATP} channel in these structures.

It was shown in ref. 11 that burst activity is correlated with a decrease in extracellular calcium. As suggested in ref. 40, the depletion of extracellular calcium would prohibit synaptic transmission, leading to alternating periods of burst and quiescence. Such a mechanism does not immediately account for features such as burst quasiperiodicity or continuous changes in BSR, nor does it provide a transparent link to the range of burst suppression etiologies. Nevertheless, aberrant calcium regulation may certainly be a companion to the mechanisms suggested in our model. Indeed, compromised brain metabolism and ATP production may impair the homeostatic neuronal pumps for maintenance of calcium levels, leading to their depletion through the course of a burst. Suppressing neuronal firing via opening of the K_{ATP} channel maximizes the energetics available for restoration of calcium.

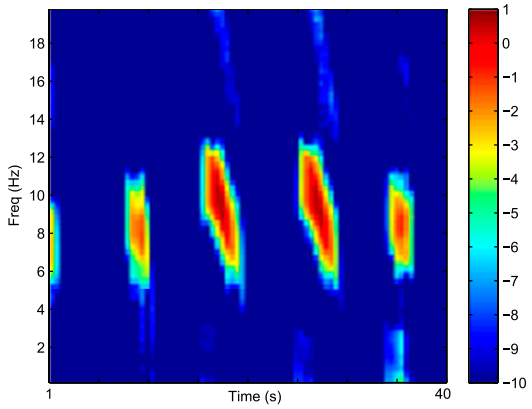

Fig. 7. Spectral drift within bursts during $J_{ATP} \times 0.3$ regime. The frequency within bursts begins around 11 Hz, is maximal at 10 Hz, and then slows to within 8 Hz before burst termination. The same phenomenon can be seen in Fig. 6*B*.

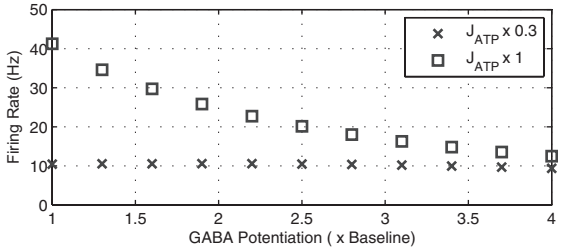

Fig. 8. Limits on high-frequency intraburst spiking. With baseline parameterization of GABA dynamics and J_{ATP}, the model can produce high-frequency gamma oscillations. As the time constant of GABA increases (longer inhibition), the firing rate in pyramidal cells decreases to the alpha range (open squares, consistent with ref. 20). When J_{ATP} is reduced by a factor of 0.3, pyramidal cell activity is restricted to the alpha range (10–12 Hz), independent of GABA dynamics.

In ref. 11, the authors also show that after the occurrence of a burst, there is a refractory period during which neural activity cannot be induced by external microstimulation. This result is again consistent with our model, in which the K_{ATP} channel remains open after cessation of spiking (due to the time constant of the gating variable z in ref. 9) (Fig. 5). Thus, excitability of neurons is severely diminished for the period immediately following burst offset. As ATP recovers, it becomes gradually easier to initiate a burst, which may correspond to enhanced excitability (11) and higher variance in burst duration (Fig. S1).

We additionally note that the relationship between metabolism and physiological oscillations has been well studied at the level of mitochondria and cardiac dynamics (41). In this context, models have been developed that suggest how oxidative stress may lead to slow, large-amplitude oscillations and arrythmia through mechanisms that involve ATP-gated membrane channels (42). Such mechanisms are similar to those in our model for burst suppression.

Model Predictions. The model predicts the manifestation of burst suppression in scenarios involving severely compromised brain metabolism. The practice of induced hypothermia (4) during cardiac surgeries provides a powerful, parametric means of testing this mechanism. In these scenarios, we would expect burst suppression to manifest independently from the anesthetic regimen. Different anesthetic drugs may induce different spectral signatures in the EEG. Accordingly, we expect the spectral signature within a burst to be the same as that of the time period immediately preceding the onset of burst suppression.

The limitation in high-frequency activity during burst suppression may be an additional mechanism that impairs normal cortical function. This is an emergent property of the model and has not yet been investigated in experiments.

Whereas we have specifically implicated the K_{ATP} channel, it is likely that other channels may exhibit similar behavior. Moreover, the mechanism outlined herein is almost certainly related to secondary effects such as the aforementioned regulation of extracellular calcium. The autoregulation of physiological processes such as cerebral blood flow may also be important in burst suppression (39, 43).

The present model does not possess the spatial scale to describe the relationship between disparate brain regions during burst suppression. However, on the basis of the model, we anticipate some degree of variation due to regional metabolic differences.

Relationship with Other Slow Activity Brain Development. Burst suppression is different from slow-wave activity in general anesthesia or sleep. Slow oscillations are thought to be spatially

local, both in cortical location and in depth (44, 45), and occur on a timescale that is faster than that of burst suppression. Moreover, burst suppression does not appear in normal sleep (2). From our model, we anticipate that these oscillations are recovered during bursts.

A phenomenon that may also be related to our model is the so-called *trace alternant*—a burst suppression-like EEG pattern—observed in some healthy newborns (46). The mechanism of our model implies that burst suppression is a means of cell preservation, allocating maximum energetics for basic cell functions, thus preventing collapse of membrane potential in low metabolic states. Similarly, the *trace alternant* may be associated with optimal brain energetics in the absence of higher-order functions during early development.

Clinical Interpretations and Potential Implications. The mechanisms of burst suppression presented here reveal the hierarchy in which neural activity is abolished in states of severely reduced brain function. Each successive burst can be viewed as an attempted recovery of basal cortical dynamics. Suppression ensues when there is an imbalance in neuronal activity and available energetics. In extreme cases, such as ischemia, even complete isoelectricity may not preserve ATP reserves, leading to eventual brain damage.

These mechanisms have potential implications for brain monitoring and intraoperative care. For instance, a detailed characterization of the burst suppression pattern may enable the detection of cerebral ischemia during surgery (47), perhaps through a change in the spectral characteristic within bursts. Such characterization may also help to differentiate "bursting" in an inactivated brain versus one in a state of seizure (9, 40).

Burst suppression is often used as a target in medically induced coma for brain protection during intensive care (3). The model provides further justification for this technique and may eventually help design paradigms for optimally achieving this brain state using anesthetic drugs and/or hypothermia. For instance, clarifying the metabolic differences between a low BSR—say, a few short bursts per minute—and complete isoelectricity would help refine targets for neuroprotection.

Finally, the model provides a means to explore new therapeutic strategies and pharmacology. It has been reported in animal studies that pyruvate may prolong neural survival during ischemic infarctions (48, 49). Pyruvate is known to stabilize oxidative metabolism by increasing ATP production during hypoxic events. Our model suggests that such an effect should manifest in terms of the BSR—a clinically relevant and testable hypothesis.

ACKNOWLEDGMENTS. This study was supported by National Institutes of Health Grants DP1-OD003646, K25-NS057580, and DP2-OD006454 and National Science Foundation Grants DMS-1042134 and DMS-0717670.

1. Swank RL, Watson CW (1949) Effects of barbiturates and ether on spontaneous electrical activity of dog brain. *J Neurophysiol* 12:137–160.
2. Brown EN, Lydic R, Schiff ND (2010) General anesthesia, sleep, and coma. *N Engl J Med* 363:2638–2650.
3. Marion DW, et al. (1997) Treatment of traumatic brain injury with moderate hypothermia. *N Engl J Med* 336:540–546.
4. Stecker MM (2007) Neurophysiology of surgical procedures for repair of the aortic arch. *J Clin Neurophysiol* 24:310–315.
5. Stecker MM, et al. (2001) Deep hypothermic circulatory arrest: II. Changes in electroencephalogram and evoked potentials during rewarming. *Ann Thorac Surg* 71:22–28.
6. Young GB (2000) The EEG in coma. *J Clin Neurophysiol* 17:473–485.
7. Ohtahara S, Yamatogi Y (2006) Ohtahara syndrome: With special reference to its developmental aspects for differentiating from early myoclonic encephalopathy. *Epilepsy Res* 70(Suppl 1):S58–S67.
8. Ohtahara S, Yamatogi Y (2003) Epileptic encephalopathies in early infancy with suppression-burst. *J Clin Neurophysiol* 20:398–407.
9. Brenner RP (1985) The electroencephalogram in altered states of consciousness. *Neurol Clin* 3:615–631.
10. Steriade M, Amzica F, Contreras D (1994) Cortical and thalamic cellular correlates of electroencephalographic burst-suppression. *Electroencephalogr Clin Neurophysiol* 90:1–16.
11. Kroeger D, Amzica F (2007) Hypersensitivity of the anesthesia-induced comatose brain. *J Neurosci* 27:10597–10607.
12. Ferron JF, Kroeger D, Chever O, Amzica F (2009) Cortical inhibition during burst suppression induced with isoflurane anesthesia. *J Neurosci* 29:9850–9860.
13. Rae-Grant AD, Kim YW (1994) Type III intermittency: A nonlinear dynamic model of EEG burst suppression. *Electroencephalogr Clin Neurophysiol* 90:17–23.
14. Henry CE, Scoville WB (1952) Suppression-burst activity from isolated cerebral cortex in man. *Electroencephalogr Clin Neurophysiol* 4:1–22.
15. Lazar LM, Milrod LM, Solomon GE, Labar DR (1999) Asynchronous pentobarbital-induced burst suppression with corpus callosum hemorrhage. *Clin Neurophysiol* 110(6): 1036–1040.
16. Vijn PC, Sneyd JR (1998) I.v. anaesthesia and EEG burst suppression in rats: Bolus injections and closed-loop infusions. *Br J Anaesth* 81:415–421.
17. Bauer G, Niedermeyer E (1979) Acute convulsions. *Clin Electroencephalogr* 10:127–144.
18. Purdon PL, et al. (2009) Simultaneous electroencephalography and functional magnetic resonance imaging of general anesthesia. *Ann N Y Acad Sci* 1157:61–70.
19. Cimenser A, et al. (2011) Tracking brain states under general anesthesia by using global coherence analysis. *Proc Natl Acad Sci USA* 108:8832–8837.
20. Ching S, Cimenser A, Purdon PL, Brown EN, Kopell NJ (2010) Thalamocortical model for a propofol-induced alpha-rhythm associated with loss of consciousness. *Proc Natl Acad Sci USA* 107:22665–22670.
21. Brown EN, Purdon PL, Van Dort CJ (2011) *Annu Rev Neurosci* 34:601–628.
22. Edgren E, et al. (2003) Cerebral blood flow and metabolism after cardiopulmonary resuscitation. A pathophysiologic and prognostic positron emission tomography pilot study. *Resuscitation* 57:161–170.
23. Williams AN, Gray RG, Poulton K, Ramani P, Whitehouse WP (1998) A case of Ohtahara syndrome with cytochrome oxidase deficiency. *Dev Med Child Neurol* 40:568–570.
24. Levy WJ, Pantin E, Mehta S, McGarvey M (2003) Hypothermia and the approximate entropy of the electroencephalogram. *Anesthesiology* 98:53–57.
25. Hirsch N, Taylor C (2010) Pharmacological and pathological modulation of cerebral physiology. *Anaesth Intensive Care Med* 11:349–354.
26. Barash PG, et al. (2009) *Clinical Anesthesia* (Lippincott Williams & Wilkins, Philadelphia), 6th Ed.
27. Murdoch J, Hall R (1990) Brain protection: Physiological and pharmacological considerations. Part I: The physiology of brain injury. *Can J Anaesth* 37:663–671.
28. Wang L, et al. (2011) The protective roles of mitochondrial ATP-sensitive potassium channels during hypoxia-ischemia-reperfusion in brain. *Neurosci Lett* 491:63–67.
29. Cunningham MO, et al. (2006) Neuronal metabolism governs cortical network response state. *Proc Natl Acad Sci USA* 103:5597–5601.
30. Dayan P, Abbott LF (2005) *Theoretical Neuroscience* (MIT Press, Cambridge, MA).
31. Du F, et al. (2008) Tightly coupled brain activity and cerebral ATP metabolic rate. *Proc Natl Acad Sci USA* 105:6409–6414.
32. Lin AL, Fox PT, Hardies J, Duong TQ, Gao JH (2010) Nonlinear coupling between cerebral blood flow, oxygen consumption, and ATP production in human visual cortex. *Proc Natl Acad Sci USA* 107:8446–8451.
33. Attwell D, Laughlin SB (2001) An energy budget for signaling in the grey matter of the brain. *J Cereb Blood Flow Metab* 21:1133–1145.
34. Loussouarn G, Pike LJ, Ashcroft FM, Makhina EN, Nichols CG (2001) Dynamic sensitivity of ATP-sensitive K(+) channels to ATP. *J Biol Chem* 276:29098–29103.
35. Milde LN (1992) Clinical use of mild hypothermia for brain protection: A dream revisited. *J Neurosurg Anesthesiol* 4:211–215.
36. Oshima T, Karasawa F, Satoh T (2002) Effects of propofol on cerebral blood flow and the metabolic rate of oxygen in humans. *Acta Anaesthesiol Scand* 46:831–835.
37. McCarthy MM, Brown EN, Kopell NJ (2008) Potential network mechanisms mediating electroencephalographic beta rhythm changes during propofol-induced paradoxical excitation. *J Neurosci* 28:13488–13504.
38. Börgers C, Epstein S, Kopell NJ (2005) Background gamma rhythmicity and attention in cortical local circuits: A computational study. *Proc Natl Acad Sci USA* 102:7002–7007.
39. van Alfen N, van Hal M, Karmann C (2011) Coupling between electroencephalography pattern and cyclic transcranial Doppler flow during aortic root surgery. *J Neurosurg Anesthesiol* 23:55–56.
40. Amzica F (2009) Basic physiology of burst-suppression. *Epilepsia* 50(Suppl 12):38–39.
41. Aon MA, Cortassa S, O'Rourke B (2008) Mitochondrial oscillations in physiology and pathophysiology. *Adv Exp Med Biol* 641:98–117.
42. Zhou L, et al. (2009) Modeling cardiac action potential shortening driven by oxidative stress-induced mitochondrial oscillations in guinea pig cardiomyocytes. *Biophys J* 97: 1843–1852.
43. Liu X, Zhu XH, Zhang Y, Chen W (2011) Neural origin of spontaneous hemodynamic fluctuations in rats under burst-suppression anesthesia condition. *Cereb Cortex* 21: 374–384.
44. Csercsa R, et al. (2010) Laminar analysis of slow wave activity in humans. *Brain* 133: 2814–2829.
45. Nir Y, et al. (2011) Regional slow waves and spindles in human sleep. *Neuron* 70: 153–169.
46. Thordstein M, et al. (2004) Spectral analysis of burst periods in EEG from healthy and post-asphyctic full-term neonates. *Clin Neurophysiol* 115:2461–2466.
47. Cohn L (2007) *Cardiac Surgery in the Adult* (McGraw-Hill Professional, New York), 3rd Ed.
48. Mongan PD, Capacchione J, Fontana JL, West S, Bünger R (2001) Pyruvate improves cerebral metabolism during hemorrhagic shock. *Am J Physiol Heart Circ Physiol* 281: H854–H864.
49. Mongan PD, Fontana JL, Chen R, Bünger R (1999) Intravenous pyruvate prolongs survival during hemorrhagic shock in swine. *Am J Physiol* 277:H2253–H2263.